

Short communication

Degradation of polymer electrolyte fuel cells under the existence of anion species

Koji Matsuoka*, Shigeru Sakamoto, Kunihiro Nakato, Akira Hamada, Yasuhiko Itoh

R&D H.Q., SANYO Electric Co., Ltd., 1-1-1 Sakata Oizumi-Machi, Ora-gun Gunma 370-0596, Japan

Received 5 November 2007; received in revised form 24 December 2007; accepted 8 January 2008

Available online 21 January 2008

Abstract

The degradation of Pt supported on carbon catalysts (Pt/C) due to four anion species (Cl^- , F^- , SO_4^{2-} , NO_3^-) was investigated by operation tests using single cells of a polymer electrolyte fuel cell (PEFC). A loss of cell voltage and of electrochemical surface area (ECA) of the cathode catalyst, and an increase in oxygen gain were shown only when a solution containing Cl^- was supplied. Scanning electron microscope (SEM) and transmission electron microscope (TEM) analysis after 50 h tests showed partial Pt dissolution and deposition in the membrane (Pt band) only in the inlet-side of the membrane electrode assembly (MEA). The partial loss of Pt led to the concentration of current density and degradation of cell performances.

© 2008 Elsevier B.V. All rights reserved.

Keywords: Fuel cells; Catalyst; Platinum; Single cell test; Impurity anion; Chloride ion

1. Introduction

Polymer electrolyte fuel cells (PEFCs) are future energy sources of great promise. They convert chemical energy to electrical energy with a significantly greater efficiency than conventional combustion processes and are environmentally friendly. We have been developing residential 1 kW co-generation systems of PEFCs [1] and participating in the large scale monitoring tests (ca. 300 systems year⁻¹) sponsored by the New Energy Foundation (NEF). To be commercially successful, cost and durability are most important considerations. There is, however, limited current information available on the failure modes of PEFCs, and the causes and mechanisms of degradation have not yet been clarified.

The degradation of catalysts is one of the most important issues associated with PEFCs. In general, both the anode and cathode catalysts are Pt or Pt-based metal alloys supported on high surface area carbon (Pt/C, Pt-M/C). The degradation of Pt/C has been reported by many researchers [2–5]. The migration [2,3] and dissolution–redeposition [4–6] of Pt have been reported as major Pt/C degradation mechanisms. Migra-

tion involves the surface diffusion of Pt, and it is accelerated by potential cycle or oxygen reduction reaction intermediates such as hydrogen peroxide [2]. The dissolution–redeposition of Pt is accelerated by potential cycles including the potential range of Pt oxide formation [4,5]. These phenomena cause the loss of electrochemical surface area (ECA) and degradation of cell performance.

On the other hand, airborne salts can be introduced into the cathode during the intake of air in PEFC operation. This is also a significant issue associated with PEFCs. The effects of anions such as Cl^- , and SO_4^{2-} in oxygen reduction and Pt dissolution have been reported. Stamenkovic et al. had reported the kinetics of the oxygen reduction reaction studied in an H_2SO_4 aqueous solution containing Cl^- on Pt(111) and Pt(100) planes [7]. The study reported that the oxygen reduction reaction is strongly inhibited on a Pt(100) surface modified by adsorbed Cl^- . Recently, the dissolution of Pt by halogen ions in H_2SO_4 solutions was reported by Yadav et al. [8]. They reported a mass loss due to the dissolution of Pt as 10 ppm chloride complexes were observed at 1.06 V (vs. SHE) through the use of an electrochemical quartz crystal microbalance and atomic force microscope. However, those experiments were only carried out with H_2SO_4 aqueous solutions or other acidic solutions. The effect of those anions in an actual MEA or PEFC cell system has not been reported to date. Therefore, cell performance due

* Corresponding author. Tel.: +81 276 61 9259; fax: +81 276 61 8896.
E-mail address: kouji.matsuoka@sanyo.com (K. Matsuoka).

to the effect of anion species such as Cl^- , F^- , SO_4^{2-} and NO_3^- was investigated by conducting operation tests using a single cell with the MEAs analyzed after the tests by microscopes in this study.

2. Experimental

2.1. Preparation of MEA

The MEA was prepared by hot pressing both the anode and the cathode catalyst onto a membrane. Both catalyst layers consisted of a catalyst and Perfluorocarbon Sulphonic Acid polymer (PFSA, Nafion[®]) electrolyte. The cathode catalyst was Pt/C (Pt 46.4%, Tanaka Kikinzoku Kogyo, Tokyo, Japan) and the anode catalyst was Pt–Ru/C (Pt 29.9%, Tanaka Kikinzoku Kogyo, Tokyo, Japan). A PFSA membrane with a thickness of 30 μm was used as an electrolyte material. The active area of the MEA was 25 cm^2 .

2.2. Single cell test

A schematic of the experimental equipment is shown in Fig. 1. A graphite plate with serpentine channel was used as the gas flow field plate. Both anode and cathode plates were tightened with stainless plates that inserted cartridge heaters (Hakko, Japan). The experiments were performed in a single cell and the current density was 0.3 A cm^{-2} . The utilizations of fuel (H_2 gas) and air were 75 and 55%, respectively. The cell temperature was 70 $^\circ\text{C}$. The gas humidification temperature was 30 $^\circ\text{C}$ (cathode) and 70 $^\circ\text{C}$ (anode) and ultra-pure water or 3 mmol dm^{-3} (mM) solutions of HCl (Wako Pure Chemical Industries, reagent grade, 36%), H_2SO_4 (Wako Pure Chemical Industries, reagent grade, 98%), HF (Kishida Chemical, reagent grade, 1%), and HNO_3 (Wako Pure Chemical Industries, reagent grade, 70%) were supplied with cathode gas for 50 h. After that, solutions supply was

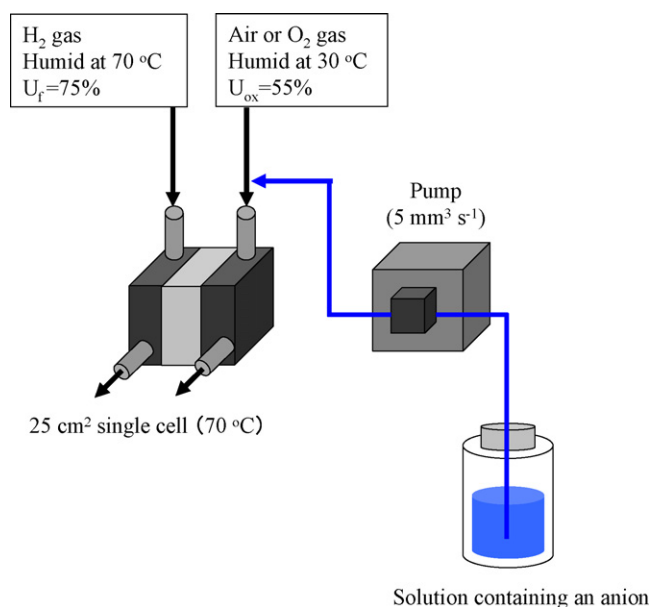


Fig. 1. Schematic illustration of fuel cell system.

terminated and the cell was operated for 24 h with both gas humidification temperatures of 70 $^\circ\text{C}$ (100%RH, normal operation). Influence of the wetting condition of MEA was minimized by 24 h operation. The cell recovered voltage was evaluated by measuring the voltage after 24 h operation. Next, the cathode gas was changed from air to oxygen and oxygen gain was calculated by determining the voltage difference between the air and oxygen (oxygen gain = $V_{\text{O}_2} - V_{\text{air}}$) [9,10].

The ECA was estimated from a cyclic voltammogram measured in H_2 (anode, 100 mL min^{-1}), N_2 (cathode, 100 mL min^{-1}) at a scan rate of 5 mV s^{-1} . The stable CVs were recorded after potential scanning for three cycles. The ECA was calculated from the electrical charge of hydrogen adsorption in the 3rd cycle.

2.3. Characterization by EPMA and TEM

Characterization of cross-sectional samples after the tests were performed using electron probe microanalysis (EPMA, EMPA1600, Shimadzu, Japan) and transmission electron microscopy (TEM, HF-2000, Hitachi, Japan).

3. Results and discussion

Fig. 2 shows the cell voltage of the supplied (a) SO_4^{2-} , (b) NO_3^- , (c) F^- , and ultra-pure water. First, solutions containing these anions were supplied to the cathode gas with air mixture for 50 h, and then normal cell operation with 100%RH gas supplied without the solution supply was carried out for 24 h to determine the degree of voltage recovery. The cell voltages were almost identical after the three anions and ultra-pure water were supplied. It showed these three anions did not influence the cell voltage. Oxygen gains of these four cells were almost identical and were ca. 80 mV. This value had not changed.

Fig. 3 shows the cell voltages of the supplied Cl^- and ultra-pure water. The cell conditions were the same as those of Fig. 2. Only the Cl^- -supplied cell showed the drop of cell voltage, and it continued to ca. 40 h. This drop in cell voltage could not be recovered back to its initial performance level after changing to normal operation. This cell voltage drop was ca. 50 mV in normal operation and oxygen gain increased to 105 mV. Prasanna et al. reported that oxygen gain was strongly associated with the mass transfer in the cathode [9,10] and that oxygen gain increased with the current density. Therefore, Cl^- was able to cause the decrease of mass transfer in the cathode.

Fig. 4 shows the cyclic voltammograms of the cathode after the 50 h operation. Fig. 5 shows the ECA change after the 50 h operation test. The vertical axis in Fig. 5 shows the initial to after-test ECA ratio. The electric double layer capacities between 400 and 500 mV, which mostly ascribed to surface area of carbon in Pt/C, were almost identical. It was suggested the degradation of carbon in Pt/C did not occur in this study. In addition, there was no change in the ECA value when ultra-pure water, SO_4^{2-} , NO_3^- and F^- were supplied. On the other hand, a decrease in current density was observed between 50 and 400 mV in a cyclic voltammogram after supplying Cl^- . The decrease in current density in this area shows the decrease in ECA. The ECA

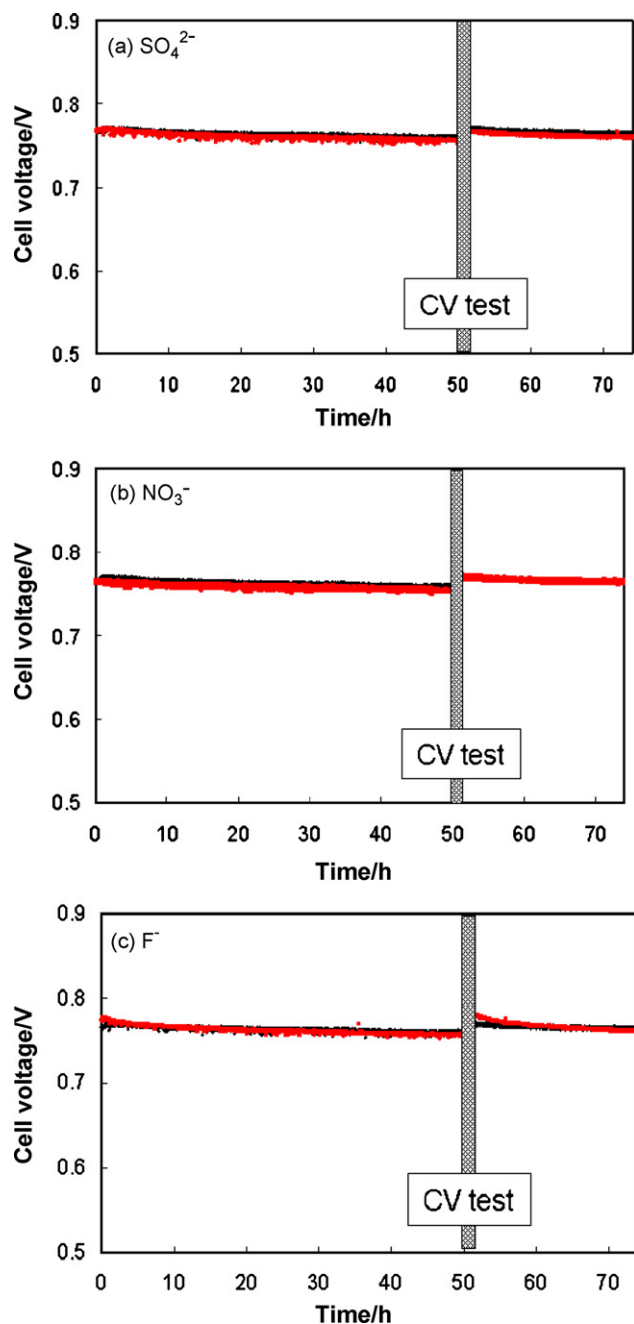
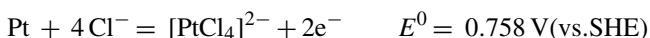


Fig. 2. Cell voltages of a PEFC single cell with 3 mM solutions of (a) SO_4^{2-} , (b) NO_3^- , (c) F^- (red line) and ultra-pure water (black line). Cell temperature: 70°C , anode humidification: 70°C , cathode humidification: 30°C and current density: 0.3 A cm^{-2} . (For interpretation of the references to colour in this figure legend, the reader is referred to the web version of the article.)

decreased to 70% of the initial ECA in the Cl^- supplying test. Yadav et al. reported that Cl^- accelerated the dissolution of Pt dissolution under a 1.06 V potential (vs. SHE) [8]. The standard electrode potentials of Pt dissolution with and without Cl^- are shown by Eqs. (1)–(3). Pt was dissolved at 758 mV (vs. SHE) and 742 mV (vs. SHE) with Cl^- , which were more negative potential than that of the case without Cl^- .



(1)

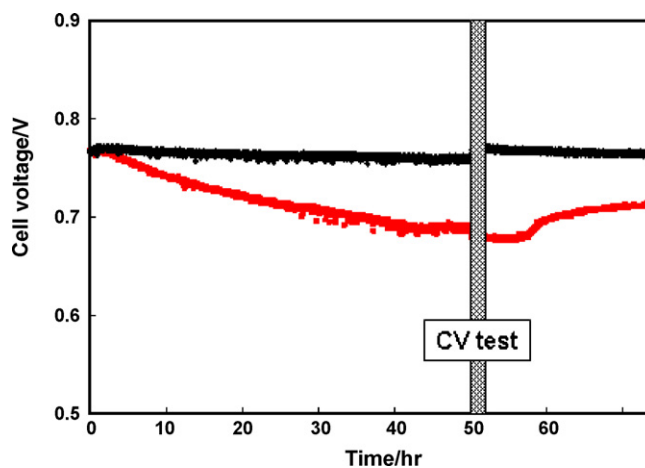


Fig. 3. Cell voltages of a PEFC single cell with 3 mM solutions of Cl^- (red line) and ultra-pure water (black line). Cell temperature: 70°C , anode humidification: 70°C , cathode humidification: 30°C and current density: 0.3 A cm^{-2} . (For interpretation of the references to colour in this figure legend, the reader is referred to the web version of the article.)

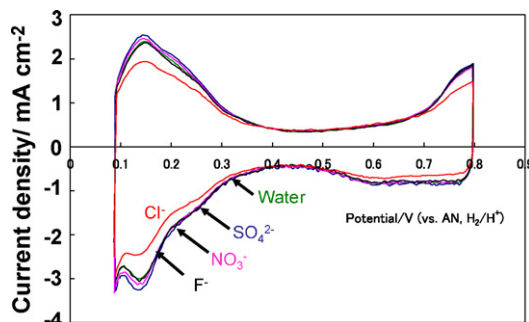
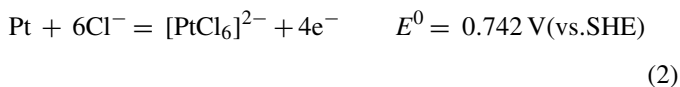
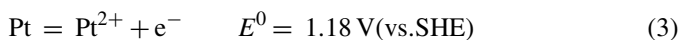


Fig. 4. Cyclic voltammograms of cathode after the test for 50 h at room temperature. Sweep rate: 5 mV s^{-1} , anode gas: H_2 and cathode gas: N_2 .



(2)



(3)

In this study, the initial cell voltage was ca. 760 mV and the cathode potential was expected to be 750–760 mV (vs. SHE). It

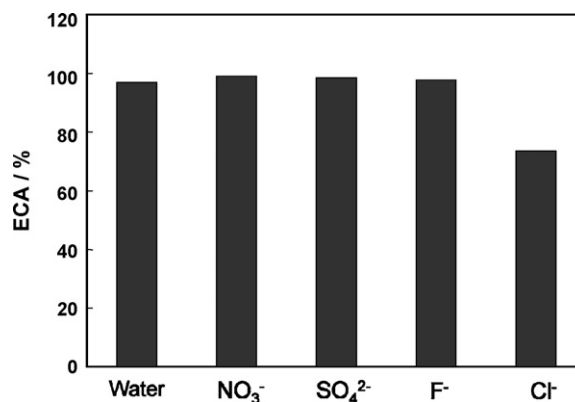


Fig. 5. Ratio of initial ECA to ECA after the 50 h operation.

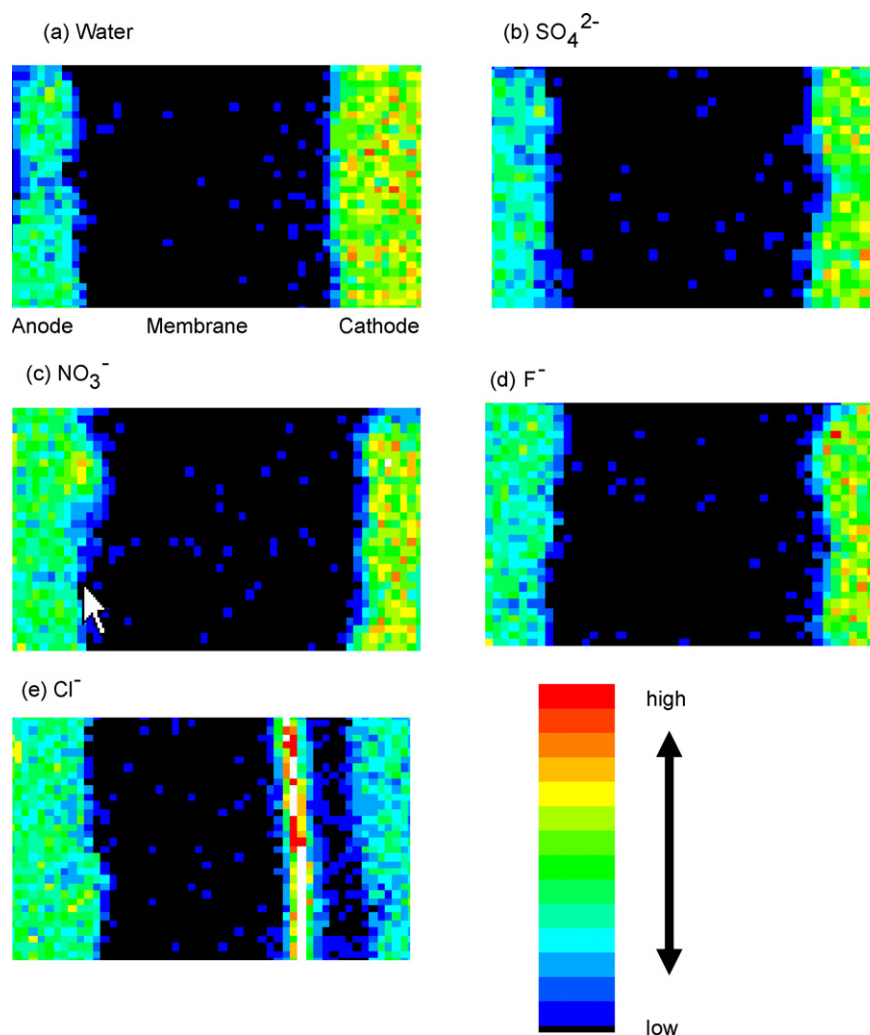


Fig. 6. EPMA images of Pt in inlet-side of MEA after the 50 h test. (a) Ultra-pure water, (b) SO_4^{2-} , (c) NO_3^- , (d) F^- and (e) Cl^- .

was suggested that a Pt catalyst could be dissolved as $[\text{PtCl}_4]^{2-}$ or $[\text{PtCl}_6]^{2-}$ under this potential with the existence of Cl^- . Although the dissolution of Pt could explain the loss of cell voltage and ECA, the cause for the oxygen gain increase had not been entirely clear. The MEA was analyzed by EPMA and TEM to clarify the increase of oxygen gain.

Fig. 6 shows the EPMA images of Pt in the inlet-side of the MEA after the test. The right and left side in these images were the anode and cathode, respectively. The images of the MEA supplying ultra-pure water (a), SO_4^{2-} (b), NO_3^- (c) and F^- (d) were almost identical and Pt was only observed in the anode and cathode. These images were also the same as those of the initial MEA (not shown). On the other hand, Pt was detected in the membrane of the MEA after supplying Cl^- . In this MEA, a large amount of Pt was deposited equidistantly from the cathode. It suggested that Pt was dissolved in the cathode catalyst layer and then deposited in the membrane. A similar phenomenon has been reported in open circuit voltage hold tests and potential cycling tests for PEFC. Ohma et al. reported Pt was deposited in the membrane by holding the open circuit voltage. The open circuit voltage hold test allowed Pt deposits to be enhanced in the membrane (Pt band) and membrane decomposition of an MEA

during an open circuit voltage due to Pt band formation [11]. Bi et al. reported that the Pt band was detected in the tests of potential cycling under H_2/O_2 conditions [12]. They concluded that the Pt band was formed by the reduction in the Pt ion content by H_2 crossover, and that the Pt band position could be determined by the crossover rates of hydrogen and oxygen in the membrane. In this study, metal Pt was oxidized to $[\text{PtCl}_4]^{2-}$ or $[\text{PtCl}_6]^{2-}$ by Cl^- anions and the cathode potential, then dissolved Pt ion was reduced to metal Pt by H_2 crossover and deposited in the membrane.

Fig. 7 shows the EPMA images of Pt in the (a) inlet-side, (b) middle and (c) outlet-side of the MEA after supplying Cl^- for 50 h. The Pt band was only observed in the inlet-side of the MEA. This implied that most of the Cl^- got through the inlet-side of the MEA, where the concentration of Cl^- increased and Pt catalyst was dissolved by Eqs. (1) and (2) in the early stages. In this stage, the partial loss of Pt in the inlet-side could lead the concentration of current density in the middle and outlet-sides of the MEA and the cell voltage decreased gradually. The concentration of Cl^- also increased in the middle and outlet-sides of MEA with time. However, Pt band could not be observed in the middle and outlet-sides of MEA, which showed no Pt dissolved in these resins. It

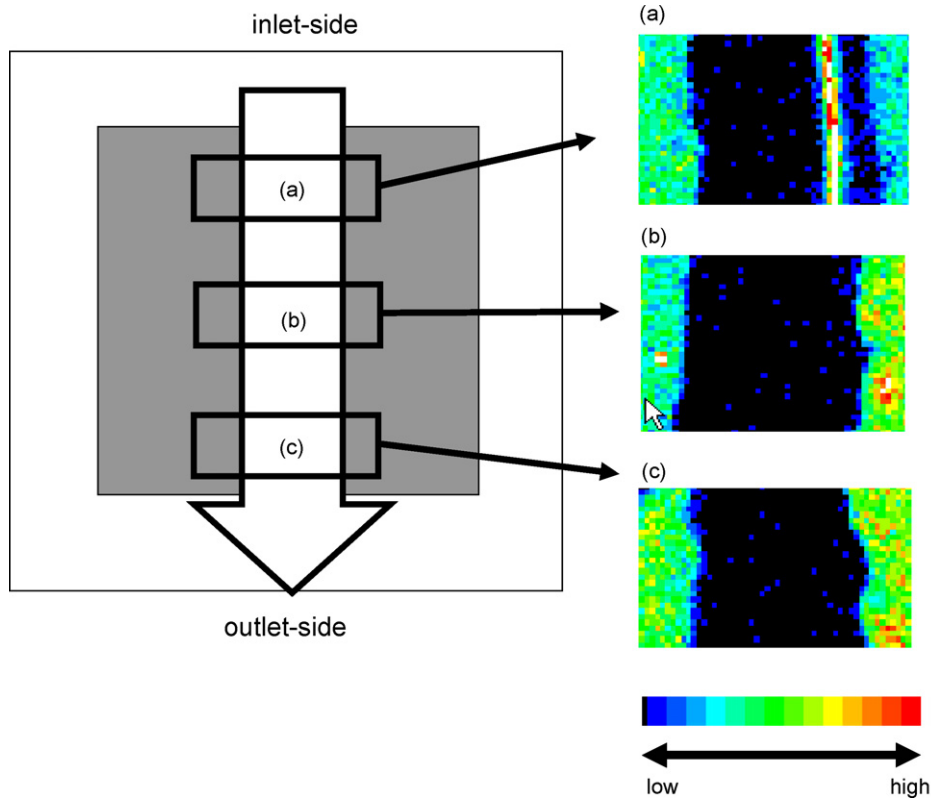


Fig. 7. EPMA images of Pt in MEA after the 50 h test. (a) Inlet-side, (b) middle side and (c) outlet-side.

was considered that the cathode potential was become too low to dissolve Pt by Eqs. (1) and (2) when the concentration of Cl^- rose enough in the middle and outlet-sides. It was implied that the increase in oxygen gain could be caused by the concentration of the current density, because increase of current density in local area had a significant effect for oxygen diffusion.

Fig. 8 shows a TEM image of the interface between the cathode catalyst layer and the membrane after supplying Cl^- for 50 h. Fig. 9 shows the average size of Pt in four regions. Zones 1–4 were shown in order near the cathode catalyst layer and zone 3 is the center of the Pt band. The Pt band was formed by a lot of Pt particles whose sizes ranged from 3 to 200 nm. Strongly

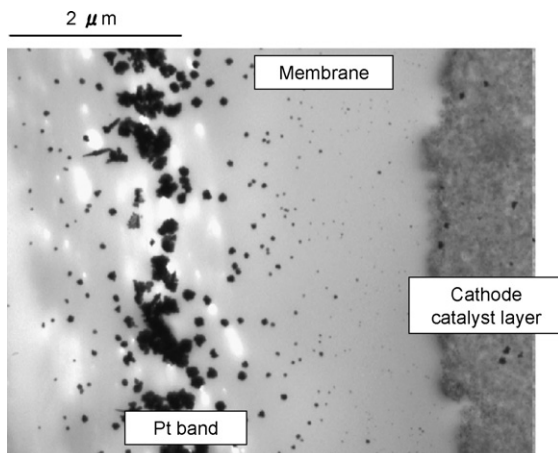


Fig. 8. TEM image of Pt at inlet-side of MEA after the 50 h test.

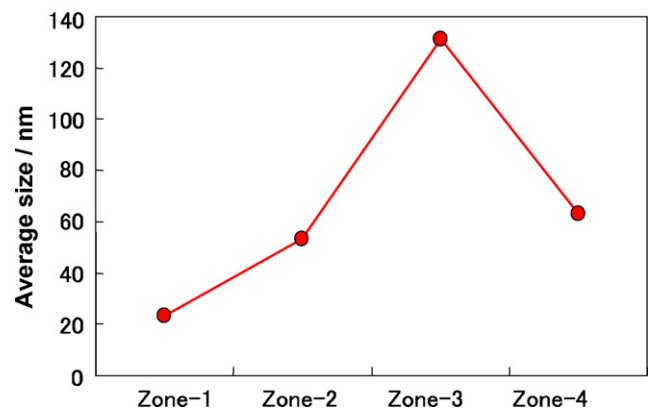
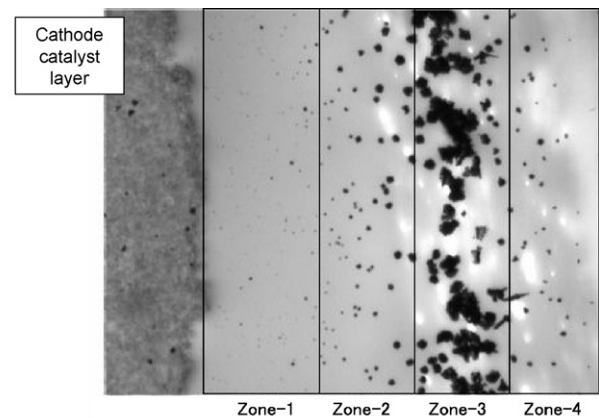


Fig. 9. The average size of Pt particles in membrane.

agglutinated Pt particles were observed around the center of the Pt band (zone 3) and the average size of Pt was ca. 135 nm. It was considered that large Pt particle in Pt band consisted of many agglutinated Pt particles.

4. Conclusions

The effects of four anion species (Cl^- , F^- , SO_4^{2-} , NO_3^-) in PEFC operation were investigated by using single cells. The three anions (F^- , SO_4^{2-} , NO_3^-) did not show effect on cell performance, and changes in MEAs could not be observed under TEM and EPMA analysis. On the other hand, Cl^- caused significant degradation in cell voltage, oxygen gain and 30% loss of ECA. Under EPMA and TEM analysis, only Cl^- promoted the dissolution of Pt in the inlet-side of the MEA and Pt particles whose sizes were 3–200 nm formed a Pt band in the membrane. The partial loss of Pt led to the concentration of current density in the middle and outlet-sides, which could cause the observed degradation of cell voltage and oxygen gain.

Acknowledgements

The authors would like to thank the New Energy and Industrial Technology Development Organization (NEDO) in their

research and development of polymer electrolyte fuel cell technology project sponsored by the Ministry of Economy, Trade and Industry, Japan.

References

- [1] T. Susai, A. Kawakami, A. Hamada, Y. Miyake, Y. Azegami, J. Power Sources 92 (2002) 131.
- [2] T. Kinumoto, K. Takai, Y. Iriyama, T. Abe, M. Inaba, Z. Ogumi, J. Electrochem. Soc. 153 (2006) A58.
- [3] K. Yasuda, A. Taniguchi, T. Akita, T. Ioroi, Z. Siroma, Phys. Chem. Chem. Phys. 8 (2006) 746.
- [4] J. Xie, D.L. Wood, K.L. More, P. Atanassov, R.L. Borup, J. Electrochem. Soc. 152 (2005) A1011.
- [5] R.M. Darling, J.P. Meyers, J. Electrochem. Soc. 150 (2003) A1523.
- [6] J. Zhang, B.A. Litteer, W. Gu, H. Liu, H.A. Gasteiger, J. Electrochem. Soc. 154 (2007) B1006.
- [7] V. Stamenkovic, N.M. Markovic, P.N. Ross Jr., J. Electroanal. Chem. 500 (2001) 44.
- [8] A.P. Yadav, A. Nishikata, T. Tsuru, Electrochim. Acta 52 (2007) 7444.
- [9] M. Prasanna, H.Y. Ha, E.A. Cho, S.-A. Hong, I.-H. Oh, J. Power Sources 137 (2004) 1.
- [10] P. Staiti, Z. Poltarzewski, V. Alderucci, G. Maggio, N. Giordano, A. Fasulo, J. Appl. Electrochem. 22 (1992) 663.
- [11] A. Ohma, S. Suga, S. Yamamoto, K. Shinohara, J. Electrochem. Soc. 154 (2007) B757.
- [12] W. Bi, G.E. Gray, T.F. Fuller, Electrochem. Solid State Lett. 10 (2007) B101.